MATCH
Communications in Mathematical and in Computer Chemistry

MATCH Commun. Math. Comput. Chem. **97** (2027) 901–922
ISSN: 0340–6253
doi: 10.46793/match.97-3.31126

Functional Quantum Calculus Approach to Degree-Based Topological Indices in Chemical Graph Theory

Shrinath Manjarekar*

Department of Mathematics and Research Center, L. V. H. Arts, Science and Commerce College (Autonomous), Nashik, India

shrimathematics@gmail.com

(Received August 26, 2026)

Abstract

In this research article, we replace the integer degree $n = \deg(v)$ of a vertex by its $q(t)$-analogue $[n]_{q(t)}$ and by an $h(t)$-analogue $\langle n\rangle_{h(t)}$ obtained from the $h(t)$-derivative of x^n at $x = 1$, and we show that every classical degree-based index $\mathrm{TI}(G) = \sum_{uv\in E(G)} F(\deg u, \deg v)$ admits two functional companions $\mathrm{TI}_{q(t)}(G)$ and $\mathrm{TI}_{h(t)}(G)$ that recover $\mathrm{TI}(G)$ exactly in the limit $t \to 0$.

We establish convergence, monotonicity, boundedness and a functional congruence theorem for these deformed indices, specialise the construction to the first and second Zagreb indices, the Randić index, the ABC index, the GA index, the harmonic index and the Sombor index, and verify all theoretical claims numerically on path, cycle, star and fused-ring (naphthalene) molecular graphs.

We then give an explicit chemical application, showing how an edge-weighted extension of the same framework tracks a degree-based topological index continuously along the reaction coordinate of a Diels–Alder cycloaddition, recovering the classical reactant- and product-graph indices at the two endpoints.

*Corresponding author.

1 Introduction

A molecule is represented in chemical graph theory by its *molecular graph*: atoms become vertices and chemical bonds become edges, usually after suppressing hydrogen atoms (the hydrogen-depleted or carbon-skeleton graph). On such a graph, the degree $\deg(v)$ of a vertex v – the number of bonds incident to the corresponding atom – is the single most informative structural quantity, and an enormous literature has grown around real-valued graph invariants, called *topological indices*, that are built purely from the degree sequence of the molecular graph and correlate, often remarkably well, with measurable physicochemical properties such as boiling point, heat of formation, strain energy, and biological activity.

The earliest and best known examples are the Wiener index [11], the Randić connectivity index [8], and the first and second Zagreb indices of Gutman and Trinajstić [3]. Later additions include the atom-bond connectivity (ABC) index [2], the geometric-arithmetic (GA) index [10], the harmonic index, and – most recently – the Sombor index [4], all of which are of the common degree-based form

$$\mathrm{TI}(G) = \sum_{uv \in E(G)} F\big(\deg(u), \deg(v)\big)$$

for a suitable two-variable function F. Deutsch and Klavzar [1] showed that essentially all such indices can be recovered, in a unified way, from a single generating function attached to the graph – the M-polynomial – by applying elementary differential and integral operators and then evaluating at $x = y = 1$. This operator calculus is the chemical graph theory analogue of generating-function techniques used throughout combinatorics and, as we exploit below, it is also the natural point of contact with q-calculus.

Every index of the above type is, however, a single number attached to a single, fixed graph. In many practically important settings – a reaction proceeding along a coordinate t, a polymer or biomolecule equilibrating at a temperature parametrised by t, a nano–structure whose effective bond pattern is perturbed continuously by an external field – one would like a continuously deformable topological descriptor: a family of numbers $\mathrm{TI}_t(G)$, indexed by a real parameter t, that reduces to the ordinary, classical $\mathrm{TI}(G)$ at a distinguished value of the parameter and varies smoothly away from it.

In the year 2024, Jafari and Manjarekar [5] introduced exactly such a one-parameter deformation mechanism at the level of quantum calculus itself. Classical $q-$ calculus and $h-$ calculus [6] replace the ordinary derivative by a difference operator governed by a single constant q (respectively h); Jafari and Manjarekar replace the constant q (respectively h) by a *function* $q(t)$ (respectively $h(t)$) of an auxiliary variable t, subject only to the natural boundary conditions $q(t) \to 1$ (respectively $h(t) \to 0$) as $t \to 0$. The resulting $q(t)$-derivative and $h(t)$-derivative reduce to the ordinary derivative exactly at $t = 0$, while for $t \neq 0$ they behave as genuine, tunable quantum-calculus operators. In particular, the $q(t)$-analogue $[n]_{q(t)}$ of a positive integer n, given in [5], is a one-parameter deformation of n itself.

The present paper exploits this single observation – that $[n]_{q(t)}$ deforms an integer while recovering it at $t = 0$ – in chemical graph theory, where the integers being deformed are precisely the vertex degrees that already drive every degree-based topological index. We replace $\deg(v)$ inside the defining sum of any degree-based index by its $q(t)$-analogue (or by an analogous $h(t)$-deformed quantity built from [5]), producing functional companions $\mathrm{TI}_{q(t)}(G)$ and $\mathrm{TI}_{h(t)}(G)$ of every classical index $\mathrm{TI}(G)$.

We show that this construction is consistent (it recovers the classical index exactly as $t \to 0$), well behaved (bounded and, under mild positivity conditions, monotone in $q(t)$), and rich enough to inherit a number-theoretic congruence property directly from [5]. We further show, that a mild edge - weighted extension of the same substitution mechanism gives a genuine chemical application: it tracks a topological index continuously as bonds actually break and form along a real reaction coordinate, rather than merely as a formal deformation of a fixed graph.

The paper is organized as follows. Section 2 collects the graph-theoretic and functional calculus preliminaries, including the relevant definitions and properties of [5] that are used later. Section 3 introduces the $q(t)-$ and $h(t)-$ deformed vertex degree and establishes its basic properties.

Section 4 defines the functional analogues of the Zagreb, Randić, ABC, GA, harmonic and Sombor indices. Section 5 proves convergence, monotonicity, boundedness and congruence theorems for these functional indices.

Section 6 verifies all of the above results to be verified for on the path graph P_5, the cycle C_6 (the benzene ring), the star $K_{1,3}$ (a branched alkane skeleton) and the fused bicyclic aromatic naphthalene. Section 7 gives an explicit chemical application to the Diels–Alder cycloaddition reaction coordinate. Section 8 discusses the chemical and physical interpretation of the parameter t, while section 9 includes the conclusion part.

2 Preliminaries

2.1 Graph-theoretic preliminaries and classical topological indices

Throughout this paper, $G = (V(G), E(G))$ denotes a finite, simple, connected graph with vertex set $V(G)$ and edge set $E(G)$, as is appropriate for a molecular (carbon-skeleton) graph. For $v \in V(G)$, $\deg(v)$ denotes its degree. For an edge $uv \in E(G)$ we write $\{\deg(u), \deg(v)\}$ for its (unordered) *degree pair*, and for $1 \leq i \leq j$ we set

$$m_{i,j}(G) = \big|\{uv \in E(G) : \{\deg(u), \deg(v)\} = \{i, j\}\}\big|,$$

so that $\{m_{i,j}(G)\}$ is the *edge partition* of G by degree pairs.

Definition 1 (M-polynomial [1])**.** The M-polynomial of G is

$$M(G; x, y) = \sum_{1 \leq i \leq j} m_{i,j}(G)\, x^i y^j.$$

All degree-based topological indices used in this paper are of the form

$$\mathrm{TI}(G) = \sum_{uv \in E(G)} F\big(\deg(u), \deg(v)\big) = \sum_{1 \leq i \leq j} m_{i,j}(G)\, F(i, j)$$

for the function F listed in Table 1.

Table 1. Classical degree-based topological indices used in this paper.

Index	Notation	$F(i,j)$
First Zagreb index [3]	$M_1(G)$	$i+j$
Second Zagreb index [3]	$M_2(G)$	$i\,j$
Randić index [8]	$R(G)$	$(i\,j)^{-1/2}$
ABC index [2]	$\mathrm{ABC}(G)$	$\sqrt{\frac{i+j-2}{i\,j}}$
GA index [10]	$\mathrm{GA}(G)$	$\frac{2\sqrt{i\,j}}{i+j}$
Harmonic index	$H(G)$	$\frac{2}{i+j}$
Sombor index [4]	$\mathrm{SO}(G)$	$\sqrt{i^2+j^2}$

2.2 Functional quantum calculus preliminaries

In this section we have given basic definitions from [5], on which the current paper were built.

Definition 2 (The set Q and H)**.** The following are the sets defined in [5] with the given conditions:

1. $\mathcal{Q} = \{\, q(t) \,:\, q(t) \to 1 \text{ as } t \to 0\}$
2. $\mathcal{H} = \{\, h(t) \,:\, h(t) \to 0 \text{ as } t \to 0\}$

Both sets are non-empty; [5].

Definition 3 (Functional $q(t)-$ and $h(t)-$ derivative)**.** Given real valued function $f(x)$ then its functional $q(t)-$ and $h(t)-$ derivatives defined by [5]:

1. $D_{q(t)}f(x) = \frac{f(q(t)x)-f(x)}{(q(t)-1)x}$
2. $D_{h(t)}f(x) = \frac{f(x+h(t))-f(x)}{h(t)}$

Property 1 ($q(t)$-analogue of n)**.** For any given positive integer n the $q(t)$-analogue of n is given by [5];

$$[n]_{q(t)} = \frac{[q(t)]^n - 1}{q(t) - 1} = 1 + q(t) + [q(t)]^2 + \cdots + [q(t)]^{n-1}.$$

Theorem 2. *If $q_1(t), q_2(t) \in \mathcal{Q}$ with $|q_1(t)| < |q_2(t)|$, then $[n]_{q_1(t)} < [n]_{q_2(t)}$ as $t \to 0$ [5].*

Theorem 3. *Let $\mathcal{Q}_1 = \{q(t) \in \mathcal{Q} : q(t) \in [0, b],\ q(t)$ continuous$\}$ and $\mathcal{H}_1 = \{h(t) \in \mathcal{H} : h(t) \in [0, b],\ h(t)$ continuous$\}$. Then $\mathcal{Q}_1$ and $\mathcal{H}_1$ are non-empty and bounded [5].*

Property 4 (Functional Quantum Congruence)**.** If $b \equiv a \pmod{m}$ then from [5], $[b]_{q(t)} \equiv [a]_{q(t)} \pmod{m}$ whenever there exists $q(t) \in \mathcal{Q}$ such that $\left|[b-a]_{q(t)} - km\right| \to 0$, for positive integers a, b, k, m.

These four statements – the analogue of an integer, its limiting growth comparison, its boundedness on a compact-parameter subclass, and its congruence behaviour – are precisely the four ingredients we use, in our next sections of this research article, to deform vertex degrees and to control the resulting topological indices.

3 Functional deformation of vertex degree

Definition 4 ($q(t)$-deformed degree)**.** Let G be a molecular graph and $v \in V(G)$ with $\deg(v) = n$. For $q(t) \in \mathcal{Q}$, the $q(t)$-deformed degree of v is

$$d_{q(t)}(v) := [n]_{q(t)} = \frac{[q(t)]^n - 1}{q(t) - 1}.$$

Definition 5 ($h(t)$-deformed degree)**.** For $h(t) \in \mathcal{H}$, the $h(t)$-deformed degree of v with $\deg(v) = n$ is

$$d_{h(t)}(v) := \langle n \rangle_{h(t)} := D_{h(t)}\big(x^n\big)\Big|_{x=1} = \frac{(1 + h(t))^n - 1}{h(t)}.$$

Definition 5 is exactly the $h(t)$-derivative of the monomial x^n, evaluated at the base point $x = 1$; the analogous classical computation, for the constant choice $h(t) = t$, already appears in [5], where it is shown directly that $D_t(x^n) \to nx^{n-1}$, and hence $D_t(x^n)|_{x=1} \to n$, as $t \to 0$ for $n \geq 1$.

Proposition 5 (Coincidence of the two deformations). *If $q(t) = 1 + h(t)$ for some $h(t) \in \mathcal{H}$, then $d_{q(t)}(v) = d_{h(t)}(v)$ for every vertex v.*

Proof. With $q(t) = 1+h(t)$ we have $q(t)-1 = h(t)$ and $[q(t)]^n = (1+h(t))^n$, so Definition 4 reads $d_{q(t)}(v) = \big((1 + h(t))^n - 1\big)/h(t)$, which is exactly Definition 5. ■

Proposition 5, shows that the canonical choices $q(t) = 1+t$ and $h(t) = t$ used in [5] are not two independent deformations but a single one viewed through two different definitions; genuinely distinct behavior requires a $q(t)$ that is *not* of the form $1 + h(t)$, the prototype being $q(t) = e^{-t}$, already used as a contrasting example in [5].

Lemma 1 (Invariance of Pendant vertices). *For every $q(t) \in \mathcal{Q}$ and every $h(t) \in \mathcal{H}$, a vertex of degree 1 satisfies $d_{q(t)}(v) = 1$ and $d_{h(t)}(v) = 1$ identically in t.*

Proof. With $n = 1$, $[1]_{q(t)} = ([q(t)]^1 - 1)/(q(t) - 1) = 1$ and $\langle 1\rangle_{h(t)} = ((1 + h(t)) - 1)/h(t) = 1$ for every admissible $q(t), h(t)$. ■

Lemma 1 has an immediate chemical reading: terminal (pendant) atoms – methyl groups, terminal halogens, single-bonded substituents – contribute to every functional topological index in exactly the same, undeformed way as in the classical theory; only atoms of degree ≥ 2 (ring and branch atoms) are sensitive to the deformation parameter t. We will verify this numerically in Section 6.

Lemma 2 (Limiting behavior). *For every vertex v with* $\deg(v) = n$*, $d_{q(t)}(v) \to n$ as $t \to 0$ and $d_{h(t)}(v) \to n$ as $t \to 0$.*

Proof. By using the above property, $[n]_{q(t)} = \sum_{k=0}^{n-1}[q(t)]^k$ is a finite sum of n terms, each of which tends to 1 as $t \to 0$ because $q(t) \to 1$; hence $[n]_{q(t)} \to n$. For the $h(t)$-deformed degree, the binomial theorem gives

$$(1+h(t))^n - 1 = n\,h(t) + \tbinom{n}{2}h(t)^2 + \cdots + h(t)^n$$

Hence it gives finally as;

$$\langle n\rangle_{h(t)} = n + \tbinom{n}{2}h(t) + \cdots + h(t)^{n-1} \to n \text{ as } h(t) \to 0$$

as $t \to 0$. ■

Lemma 3 (Boundedness)**.** *If $q(t) \in \mathcal{Q}_1$, then for every vertex v of a finite graph G, $d_{q(t)}(v)$ is bounded, uniformly over t in the domain of $q(t)$.*

Proof. Since $q(t) \in [0,b]$, each power $[q(t)]^k$, $k = 0,\ldots,n-1$, lies in $[0,b^k]$, so the finite sum defining $[n]_{q(t)}$ lies in $[0, 1+b+\cdots+b^{n-1}]$, a bound depending only on $n = \deg(v)$ and b. As G is finite, the maximum degree $\Delta(G)$ is finite.

Hence,

$$d_{q(t)}(v) \leq 1 + b + \cdots + b^{\Delta(G)-1}$$

for every $v \in V(G)$. ■

4 Functional topological indices

We now use Definitions 4 and 5 to deform every index of Table 1.

Definition 6 (Master definition)**.** Let $\mathrm{TI}(G) = \sum_{uv\in E(G)} F(\deg u, \deg v)$ be a classical degree-based topological index. Its $q(t)$-functional analogue and $h(t)$-functional analogue are

1. $\mathrm{TI}_{q(t)}(G) = \sum_{uv\in E(G)} F\big(d_{q(t)}(u),\, d_{q(t)}(v)\big)$
2. $\mathrm{TI}_{h(t)}(G) = \sum_{uv\in E(G)} F\big(d_{h(t)}(u),\, d_{h(t)}(v)\big)$

Equivalently, in terms of the edge partition,

1. $\mathrm{TI}_{q(t)}(G) = \sum_{1\leq i\leq j} m_{i,j}(G)\, F\big([i]_{q(t)}, [j]_{q(t)}\big)$
2. $\mathrm{TI}_{h(t)}(G) = \sum_{1\leq i\leq j} m_{i,j}(G)\, F\big(\langle i\rangle_{h(t)}, \langle j\rangle_{h(t)}\big)$

Specializing F as in Table 1 produces the functional indices collected in Table 2 (writing only the $q(t)-$ version; the $h(t)-$ version is obtained by replacing every $[\cdot]_{q(t)}$ with $\langle\cdot\rangle_{h(t)}$).

Table 2. Functional ($q(t)-$ deformed) degree-based topological indices

Index	Definition
$M_{1,q(t)}(G)$	$\sum_{1\leq i\leq j} m_{i,j}(G)\big([i]_{q(t)}+[j]_{q(t)}\big)$
$M_{2,q(t)}(G)$	$\sum_{1\leq i\leq j} m_{i,j}(G)\,[i]_{q(t)}[j]_{q(t)}$
$R_{q(t)}(G)$	$\sum_{1\leq i\leq j} m_{i,j}(G)\big([i]_{q(t)}[j]_{q(t)}\big)^{-1/2}$
$\mathrm{ABC}_{q(t)}(G)$	$\sum_{1\leq i\leq j} m_{i,j}(G)\sqrt{\frac{[i]_{q(t)}+[j]_{q(t)}-2}{[i]_{q(t)}[j]_{q(t)}}}$
$\mathrm{GA}_{q(t)}(G)$	$\sum_{1\leq i\leq j} m_{i,j}(G)\frac{2\sqrt{[i]_{q(t)}[j]_{q(t)}}}{[i]_{q(t)}+[j]_{q(t)}}$
$H_{q(t)}(G)$	$\sum_{1\leq i\leq j} m_{i,j}(G)\frac{2}{[i]_{q(t)}+[j]_{q(t)}}$
$\mathrm{SO}_{q(t)}(G)$	$\sum_{1\leq i\leq j} m_{i,j}(G)\sqrt{[i]_{q(t)}^2+[j]_{q(t)}^2}$

Remark. Definition 6 requires no new computational machinery beyond the Property of $q-$ analogue of n and the $h(t)-$ derivative of x^n at $x=1$: every functional index is obtained from its classical counterpart by the single, uniform substitution $i\mapsto[i]_{q(t)}$ (or $i\mapsto\langle i\rangle_{h(t)}$) inside the edge-partition sum.

This is the chemical-graph-theory counterpart of the operator calculus of Deutsch and Klavzar [1]: there, classical indices are recovered from the M-polynomial by differential/integral operators that act on a monomial x^iy^j as multiplication by i (or j, or $1/i$, etc.); here, the same monomial is acted on by multiplication by $[i]_{q(t)}$, which is precisely the eigenvalue produced by the $q(t)$-derivative operator $D_{q(t)}$ of [5] acting on x^i at $x = 1$, since $D_{q(t)}(x^i)\big|_{x=1} = \big([q(t)]^i - 1\big)/(q(t) - 1) = [i]_{q(t)}$.

5 Theoretical results

Theorem 6 (Convergence Theorem)**.** *For every degree-based index* TI *with continuous F, and every finite graph G,*

$$\lim_{t\to 0} \mathrm{TI}_{q(t)}(G) = \mathrm{TI}(G) \qquad \textit{and} \qquad \lim_{t\to 0} \mathrm{TI}_{h(t)}(G) = \mathrm{TI}(G).$$

Proof. G is finite, so the sum in Definition 6 has finitely many terms. By Lemma 2, $[i]_{q(t)} \to i$ and $[j]_{q(t)} \to j$ as $t \to 0$ for every pair (i, j) occurring in the edge partition of G; since F is continuous, $F([i]_{q(t)}, [j]_{q(t)}) \to F(i, j)$. A finite sum of convergent terms converges to the sum of the limits, giving $\mathrm{TI}_{q(t)}(G) \to \sum_{i\le j} m_{i,j}(G)F(i, j) = \mathrm{TI}(G)$. The $h(t)$-case is identical, using the second part of Lemma 2. ■

Theorem 7 (Boundedness Theorem)**.** *If $q(t) \in \mathcal{Q}_1$ in the sense of Theorem 3 and F is continuous, then $\mathrm{TI}_{q(t)}(G)$ is bounded, uniformly in t, for every finite graph G.*

Proof. By Lemma 3, every deformed degree $d_{q(t)}(v)$ lies in a compact interval $[1, M]$ depending only on $\Delta(G)$ and the bound b of $\mathcal{Q}_1$. A continuous function F is bounded on the compact set $[1, M] \times [1, M]$, so each of the finitely many terms $F(d_{q(t)}(u), d_{q(t)}(v))$ in Definition 6 is bounded uniformly in t, and hence so is their (finite) sum. ■

Theorem 8 (Monotonicity of the Zagreb-type functional indices)**.** *Let $q_1(t), q_2(t) \in \mathcal{Q}$ satisfy $0 < q_1(t) < q_2(t)$. Then for every finite graph G,*

$$M_{1,q_1(t)}(G) \le M_{1,q_2(t)}(G) \quad \textit{and} \quad M_{2,q_1(t)}(G) \le M_{2,q_2(t)}(G)$$
$$\textit{as } t \to 0,$$

while the Randić-type functional index satisfies the reverse inequality,

$$R_{q_1(t)}(G) \geq R_{q_2(t)}(G) \quad \textit{as } t \to 0.$$

Proof. Under the stated positivity hypothesis, $0 < q_1(t) < q_2(t)$ in particular gives $|q_1(t)| < |q_2(t)|$, so Theorem 2 applies term-by-term to every degree n occurring in G: $[n]_{q_1(t)} < [n]_{q_2(t)}$ as $t \to 0$. Since $F(i,j) = i + j$ and $F(i,j) = ij$ are both increasing in each non-negative argument, replacing every $[i]_{q_1(t)}, [j]_{q_1(t)}$ by the larger $[i]_{q_2(t)}, [j]_{q_2(t)}$ in Definition 6 cannot decrease any term of the (non-negative) edge-partition sum, which gives the first two inequalities. For the Randić-type index, $F(i,j) = (ij)^{-1/2}$ is decreasing in each argument, so the same substitution reverses the inequality. ■

Corollary. *For a Δ-regular molecular graph G (every vertex of the same degree Δ, as in benzenoid rings or fullerene cages), the chain of inequalities in Theorem 8 reduces to a strict, totally ordered family $M_{1,q(t)}(G) = |E(G)| \cdot 2[\Delta]_{q(t)}$, strictly increasing in $q(t)$ on $(0, \infty)$ for $\Delta \geq 2$.*

Theorem 9 (Functional Quantum Congruence for Isodegree Graphs)**.** *Let G_1, G_2 be finite graphs whose edge-partition degree pairs are congruent modulo a fixed positive integer m, i.e. for every pair (i_1, j_1) occurring in G_1 there is a corresponding pair (i_2, j_2) occurring in G_2 with $i_1 \equiv i_2 \pmod{m}$ and $j_1 \equiv j_2 \pmod{m}$, and with matching multiplicities $m_{i_1,j_1}(G_1) = m_{i_2,j_2}(G_2)$. Then, whenever there exists $q(t) \in \mathcal{Q}$ satisfying the limiting condition of Property 4 for each such pair, the term-wise deformed degrees satisfy*

$$[i_1]_{q(t)} \equiv [i_2]_{q(t)} \pmod{m} \textit{ and } [j_1]_{q(t)} \equiv [j_2]_{q(t)} \pmod{m}, \textit{ and}$$

consequently it gives us;

$$M_{1,q(t)}(G_1) \equiv M_{1,q(t)}(G_2) \pmod{m}$$

Proof. Property 4 gives $[i_1]_{q(t)} \equiv [i_2]_{q(t)} \pmod{m}$ from $i_1 \equiv i_2 \pmod{m}$ (and likewise for j_1, j_2), under the stated limiting condition on $q(t)$. Summing $\left([i_1]_{q(t)} + [j_1]_{q(t)}\right) \equiv \left([i_2]_{q(t)} + [j_2]_{q(t)}\right) \pmod{m}$ over the matched, equally multiplicities edge classes preserves the congruence, since a finite sum of congruent terms is congruent modulo m. ■

6 Numerical computations

In this section, we will verify Theorems 6 and 8 on four molecular graphs of increasing complexity, using the two canonical deformation functions of [5]: $q(t) = 1 + t$ (which, by Proposition 5, coincides with the $h(t) = t$ deformation) and the genuinely different choice $q(t) = e^{-t}$. All numerical values below were computed symbolically and verified to 8 significant figures using scientific calculators.

6.1 Deformed degree values

Now, by Lemma 1, $[1]_{q(t)} = 1$ identically; Table 3 lists $[2]_{q(t)}$ and $[3]_{q(t)}$, the only other degrees occurring in the examples below.

Table 3. Deformed degrees $[2]_{q(t)}$ and $[3]_{q(t)}$ for the two canonical choices of $q(t)$.

	$q(t) = 1 + t$		$q(t) = e^{-t}$	
t	$[2]_{q(t)}$	$[3]_{q(t)}$	$[2]_{q(t)}$	$[3]_{q(t)}$
0.1	2.100000	3.310000	1.904837	2.723568
0.01	2.010000	3.030100	1.990050	2.970249
0.001	2.001000	3.003001	1.999000	2.997002
$\to 0$	2	3	2	3

As already observed in [5], the two columns approach the same limits at different rates: for $q(t) = 1 + t$ the deformed degree overshoots the classical value from above, while for $q(t) = e^{-t}$ it approaches from below.

6.2 Path graph P_5: Linear alkane backbone

We know that, a linear alkane backbone is a continuous, un–branched chain of carbon atoms connected to each other exclusively by single bonds. For example; if we consider P_5 (v_1–v_2–v_3–v_4–v_5), $\deg(v_1) = \deg(v_5) = 1$ and $\deg(v_2) = \deg(v_3) = \deg(v_4) = 2$. Then the edge partition $m_{1,2} = 2$,

$m_{2,2} = 2$. By Definition 6 and Lemma 1,

$$M_{1,q(t)}(P_5) = 2 + 6[2]_{q(t)}, \qquad M_{2,q(t)}(P_5) = 2[2]_{q(t)} + 2[2]^2_{q(t)},$$
$$R_{q(t)}(P_5) = \frac{2}{\sqrt{[2]_{q(t)}}} + \frac{2}{[2]_{q(t)}}.$$

Table 4 below reports the numerical values; the classical values are $M_1(P_5) = 14$, $M_2(P_5) = 12$, $R(P_5) = 1 + \sqrt{2} \approx 2.4142136$.

Table 4. Functional indices of P_5.

t, deformation	$M_{1,q(t)}(P_5)$	$M_{2,q(t)}(P_5)$	$R_{q(t)}(P_5)$
0.1, $q(t) = 1 + t$	14.600000	13.020000	2.3325121
0.01, $q(t) = 1 + t$	14.060000	12.100200	2.4057161
0.001, $q(t) = 1 + t$	14.006000	12.010002	2.4133604
0.1, $q(t) = e^{-t}$	13.429025	11.066486	2.4990673
0.01, $q(t) = e^{-t}$	13.940299	11.900696	2.4227446
0.001, $q(t) = e^{-t}$	13.994003	11.990007	2.4150671
$\to 0$	**14**	**12**	**2.4142136**

6.3 Cycle graph C_6: The benzene ring

We know that, a benzene ring is a fundamental cyclic hydrocarbon consisting of six carbon atoms arranged in a perfect hexagonal ring, with one hydrogen atom bonded to each carbon. This can be thought of mathematically, in terms of graph theory, as C_6, in which every vertex has degree 2, so $m_{2,2} = 6$ and

$$M_{1,q(t)}(C_6) = 12[2]_{q(t)}, \qquad M_{2,q(t)}(C_6) = 6[2]^2_{q(t)}, \qquad R_{q(t)}(C_6) = \frac{6}{[2]_{q(t)}}.$$

Table 5 below reports numerical values; classically $M_1(C_6) = 24$, $M_2(C_6) = 24$, $R(C_6) = 3$.

Table 5. Functional indices of C_6 (benzene).

t, deformation	$M_{1,q(t)}(C_6)$	$M_{2,q(t)}(C_6)$	$R_{q(t)}(C_6)$
0.1, $q(t) = 1 + t$	25.200000	26.460000	2.8571429
0.01, $q(t) = 1 + t$	24.120000	24.240600	2.9850746
0.001, $q(t) = 1 + t$	24.012000	24.024006	2.9985007
0.1, $q(t) = e^{-t}$	22.858049	21.770434	3.1498751
0.01, $q(t) = e^{-t}$	23.880598	23.761790	3.0149999
0.001, $q(t) = e^{-t}$	23.988006	23.976018	3.0015000
$\to 0$	**24**	**24**	**3**

The benzene ring example also illustrates the corollary above (Corollary 5) directly: since $\Delta = 2$ for every vertex, $M_{1,q(t)}(C_6) = 12[2]_{q(t)}$ is strictly increasing in $q(t)$ on $(0, \infty)$, exactly as predicted, and the table shows $M_{1,q(t)}(C_6) > 24$ for $q(t) = 1 + t > 1$ and $M_{1,q(t)}(C_6) < 24$ for $q(t) = e^{-t} < 1$, on either side of the classical value 24.

6.4 Star graph $K_{1,3}$: Branched alkane skeleton

We know that, a branched alkane skeleton is a hydrocarbon framework where at least one carbon atom is bonded to three or four other carbon atoms, creating side chains off the main continuous path. This can be viewed as $K_{1,3}$, which gives $m_{1,3} = 3$ and, using Lemma 1,

$$M_{1,q(t)}(K_{1,3}) = 3 + 3[3]_{q(t)}, \qquad M_{2,q(t)}(K_{1,3}) = 3[3]_{q(t)},$$
$$R_{q(t)}(K_{1,3}) = \frac{3}{\sqrt{[3]_{q(t)}}}.$$

Table 6. Functional indices of $K_{1,3}$.

t, deformation	$M_{1,q(t)}(K_{1,3})$	$M_{2,q(t)}(K_{1,3})$	$R_{q(t)}(K_{1,3})$
0.1, $q(t) = 1 + t$	12.930000	9.930000	1.6489491
0.01, $q(t) = 1 + t$	12.090300	9.090300	1.7234265
0.001, $q(t) = 1 + t$	12.009003	9.009003	1.7311851
0.1, $q(t) = e^{-t}$	11.170705	8.170705	1.8178252
0.01, $q(t) = e^{-t}$	11.910746	8.910746	1.7407037
0.001, $q(t) = e^{-t}$	11.991007	8.991007	1.7329168
$\to 0$	**12**	**9**	**1.7320508**

Table 6 gives the numerical values; classically $M_1(K_{1,3}) = 12$, $M_2(K_{1,3}) = 9$, $R(K_{1,3}) = \sqrt{3} \approx 1.7320508$.

6.5 Naphthalene

We know that, Naphthalene is the smallest fused polycyclic aromatic hydrocarbon and the natural next step beyond a single benzene ring towards extended aromatic and graphene-like lattices. Its carbon-skeleton graph has 10 vertices and 11 edges: the two bridgehead carbons have degree 3 and the remaining eight carbons have degree 2, giving the edge partition $m_{2,2} = 6$, $m_{2,3} = 4$, $m_{3,3} = 1$. Hence it gives,

1. $M_{1,q(t)} = 6\big(2[2]_{q(t)}\big) + 4\big([2]_{q(t)} + [3]_{q(t)}\big) + 1\big(2[3]_{q(t)}\big)$
2. $M_{2,q(t)} = 6[2]^2_{q(t)} + 4[2]_{q(t)}[3]_{q(t)} + 1[3]^2_{q(t)}$

and classically $M_1 = 50$, $M_2 = 57$, $R = 3 + \dfrac{4}{\sqrt{6}} + \dfrac{1}{3} \approx 4.9663265$.

Table 7 below gives the functional quantum values at $t = 0.1$ and $t = 0.01$.

Table 7. Functional indices of naphthalene.

t, deformation	$M_{1,q(t)}$	$M_{2,q(t)}$	$R_{q(t)}$
0.1, $q(t) = 1 + t$	53.460000	65.220100	4.6764350
0.01, $q(t) = 1 + t$	50.340600	57.784110	4.9359119
0.1, $q(t) = e^{-t}$	46.818808	49.940075	5.2731917
0.01, $q(t) = e^{-t}$	49.662288	56.227936	4.9969210
$\to 0$	**50**	**57**	**4.9663265**

Thus from all the above separate examples and in every one of the respective Tables 4 to 7, the entries at $t = 0.1, 0.01, 0.001$ are seen to approach the boldfaced classical limit monotonically as t decreases, confirming Theorem 6 numerically, and the $q(t) = 1 + t$ rows lie above while the $q(t) = e^{-t}$ rows lie below the classical value for M_1 and M_2, confirming the sign/ordering behavior of Theorem 8 (recall $1 + t > 1 > e^{-t}$ for $t > 0$), with the reversed ordering for the Randić index R, exactly as predicted.

7 An explicit application: the Diels–Alder reaction coordinate

The sections 3–6 deform the vertex degree of a *fixed* molecular graph. In this section, now we show that a mild, edge-weighted extension of exactly the same substitution mechanism turns this formal deformation into a genuine chemical application: it tracks a degree-based topological index continuously while two covalent bonds actually form, along the reaction coordinate of a real pericyclic reaction, the Diels–Alder $[4+2]$ cycloaddition of buta-1,3-diene with ethylene to give cyclohexene,

$$\underbrace{\mathrm{CH_2{=}CH{-}CH{=}CH_2}}_{\text{diene}} + \underbrace{\mathrm{CH_2{=}CH_2}}_{\text{dienophile}} \xrightarrow{\Delta} \text{cyclohexene.}$$

This reaction is the standard textbook example of a pericyclic, concerted cycloaddition, and is particularly well suited to the present framework because it is exactly the case in which a molecular graph changes – two new σ-bonds are created simultaneously – while the atoms themselves are fixed; the classical, static theory only sees the reactant graph and the product graph, at the two ends of the reaction, and cannot describe anything in between.

7.1 Labelling and the two static endpoints

Label the diene carbons C_1–C_2–C_3–C_4 (with double bonds $C_1{=}C_2$ and $C_3{=}C_4$) and the ethylene carbons C_5–C_6 (double bond $C_5{=}C_6$). In the carbon-skeleton (simple) graph, the reactant state is the disjoint union $P_4 \cup P_2$, with degree sequence $\deg(C_1) = \deg(C_4) = \deg(C_5) = \deg(C_6) = 1$ and $\deg(C_2) = \deg(C_3) = 2$; in Section 4, this is exactly the edge partition $m_{1,2} = 2$, $m_{2,2} = 1$ (for P_4) together with the single edge $m_{1,1} = 1$ (for P_2), giving classical values

$$M_1(\text{reactants}) = 10 + 2 = 12, \qquad M_2(\text{reactants}) = 8 + 1 = 9.$$

In the concerted mechanism, new σ-bonds form between C_1 and C_6 and between C_4 and C_5, while the double bond migrates from $C_1 = C_2/C_3 = C_4$ to $C_2 = C_3$; the product carbon skeleton is the 6-cycle C_6 visited in the order C_1-C_2-C_3-C_4-C_5-C_6-C_1. Every vertex of this ring has degree 2, so it is degree-wise identical to the benzene ring already analysed in Section 6.3, and

$$M_1(\text{cyclohexene}) = 24, \qquad M_2(\text{cyclohexene}) = 24,$$
$$R(\text{cyclohexene}) = 3.$$

Figure 1 below displays the reactant graph, an intermediate "in-flight" state in which the two new bonds are only partially formed, and the product ring, together with the degree of the four bond-forming carbons at each stage.

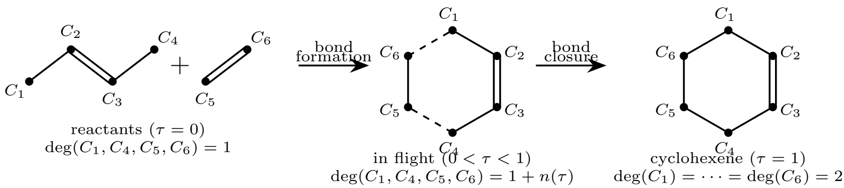

Figure 1. The Diels–Alder cycloaddition read as a continuously deformed molecular graph. Solid lines are bonds present throughout; dashed lines are the two forming σ-bonds C_1–C_6 and C_4–C_5, whose bond order $n(\tau)$ increases from 0 (reactants) to 1 (product) as the reaction progress variable τ runs from 0 to 1.

7.2 Edge – weighted extension

To interpolate between the two endpoints we extend Definition 6 by allowing each edge $e = uv$ of the *union* graph (reactant bonds together with the two forming bonds) to carry a bond-order weight $w(e) \in [0, 1]$, and by allowing the degree of a vertex to be the weighted sum of the weights of its incident edges rather than an integer count.

Definition 7 (Reaction– Coordinate Degree). Let $\tau \in [0,1]$ be the reaction progress variable from starting to end of the chemical reaction and let $n(\tau) \in [0,1]$ be a *bond-order function* with $n(0) = 0$, $n(1) = 1$, and n continuous and increasing on $[0,1]$. Assign weight 1 to every bond already present in the reactants and weight $n(\tau)$ to each of the two forming bonds. The reaction-coordinate degree of a vertex v is

$$d_\tau(v) = \sum_{e \in v} w(e),$$

the sum of the weights of the edges incident to v in the union graph, and the reaction-coordinate topological index of the master Definition 6 is

$$\mathrm{TI}_\tau(G) = \sum_{uv} w(uv)\, F\big(d_\tau(u), d_\tau(v)\big),$$

the sum now running over all edges of the union graph, each weighted by its own bond order.

By Definition 7, $d_0(C_1) = d_0(C_4) = d_0(C_5) = d_0(C_6) = 1$ (the classical reactant degrees) and $d_1(C_1) = \cdots = d_1(C_6) = 2$ (the classical product degrees), while C_2, C_3 keep degree 2 throughout, since neither is incident to a forming bond; this is exactly the pendant/ring dichotomy of Lemma 1, now transported from the t-deformation to the τ-reaction-coordinate.

Proposition 10 (Endpoint Recovery). *For every continuous bond-order function n with $n(0) = 0, n(1) = 1$,*

$$\mathrm{TI}_0(G) = M_1(\textit{reactants}) = 12, \quad \mathrm{TI}_1(G) = M_1(\textit{cyclohexene}) = 24,$$

for $F(i,j) = i + j$, and likewise $\mathrm{TI}_0(G) = 9$, $\mathrm{TI}_1(G) = 24$ for $F(i,j) = ij$.

Proof. At $\tau = 0$ the two forming bonds carry weight $n(0) = 0$ and so do not contribute to the sum in Definition 7, and every remaining weight is 1; this reduces $\mathrm{TI}_0(G)$ exactly to the classical reactant index computed in Section 7.1. At $\tau = 1$ every weight, old and new, equals 1, so $d_1(v) = \deg(v)$ in the product ring and $\mathrm{TI}_1(G)$ reduces to the classical $M_1(C_6) = 24$ (respectively $M_2(C_6) = 24$) already tabulated in Table 5. ■

Proposition 10 is the direct analogue, along the reaction coordinate τ, of the convergence Theorem 6 along the deformation parameter t: in both cases the construction is designed so that a continuous family of indices degenerates exactly to a classical, static value at a distinguished point of the parameter – here at *two* distinguished points, $\tau = 0$ and $\tau = 1$, rather than only at $t = 0$.

7.3 Explicit formulas and a smoothstep bond-order function

Writing $n = n(\tau)$ for brevity, a direct sum over the six edges of the union graph shown in Figure 1 (the four unweighted bonds C_1C_2, C_2C_3, C_3C_4, C_5C_6 and the two forming bonds C_1C_6, C_4C_5 of weight n) gives, using Definition 7,

$$M_{1,\tau}(G) = 12 + 8n + 4n^2, \qquad M_{2,\tau}(G) = 9 + 8n + 5n^2 + 2n^3.$$

Both expressions manifestly satisfy $M_{1,0} = 12$, $M_{1,1} = 24$ and $M_{2,0} = 9$, $M_{2,1} = 24$, confirming Proposition 10 algebraically. For the numerical illustration we use the classical smooth–step function

$$n(\tau) = 3\tau^2 - 2\tau^3,$$

which satisfies $n(0) = 0$, $n(1) = 1$, and has zero derivative at both endpoints – a standard, chemically reasonable choice modelling a bond order that grows slowly near the reactant and product geometries and fastest near the transition state $\tau = \frac{1}{2}$, where $n(\frac{1}{2}) = \frac{1}{2}$. Table 8 reports $M_{1,\tau}(G)$ and $M_{2,\tau}(G)$ at five values of τ.

Both $M_{1,\tau}(G)$ and $M_{2,\tau}(G)$ increase monotonically from the reactant value to the product value as τ runs from 0 to 1, since $n(\tau)$ itself is increasing and both right-hand sides above are increasing functions of $n \in [0, 1]$; this is the reaction-coordinate counterpart of the monotonicity behaviour of Theorem 8. The same substitution applies verbatim to the Randić, ABC, GA, harmonic and Sombor indices of Table 2 by replacing F in Definition 7; we have recorded only M_1 and M_2 here for brevity.

Table 8. The reaction-coordinate first and second Zagreb indices along the Diels–Alder path, using the smoothstep bond-order function $n(\tau) = 3\tau^2 - 2\tau^3$.

τ	$n(\tau)$	$M_{1,\tau}(G)$	$M_{2,\tau}(G)$
0 (reactants)	0.00000	**12.0000**	**9.0000**
0.25	0.15625	13.3477	10.3797
0.5 (transition state)	0.50000	17.0000	14.5000
0.75	0.84375	21.5977	20.5110
1 (cyclohexene)	1.00000	**24.0000**	**24.0000**

8 Chemical and physical interpretation

The parameter t in $\mathrm{TI}_{q(t)}(G)$ and $\mathrm{TI}_{h(t)}(G)$ has no analogue in the classical theory, where a topological index is computed once and for all from the static molecular graph. The functional framework of Sections 3 to 5 suggests at least three readings of t that are natural in applications.

(i) Reaction coordinate

If G models a transition-state or intermediate structure along a reaction path parametrised by $t \in [0, 1]$ (with $t = 0$ the reactant and $t = 1$ the product), $\mathrm{TI}_{q(t)}(G)$ provides a continuously varying structural descriptor along the path, rather than the two static endpoint values used in conventional QSPR/QSAR studies. Section 7 makes this reading fully explicit and quantitative for the Diels–Alder cycloaddition, where the reactant and product values recovered at $\tau = 0, 1$ in Proposition 10 are precisely the two classical endpoint values that the static theory is confined to.

(ii) Temperature or vibrational amplitude

Bond lengths and effective coordination numbers in a real molecule fluctuate with temperature; treating t as proportional to a reduced temperature (or to a thermal expansion parameter) and choosing $q(t)$ to model the empirically observed bond-order softening gives a temperature-dependent topological index $\mathrm{TI}_{q(t)}(G)$ whose $t \to 0$ limit is the index computed from the equilibrium (zero-temperature) graph, consistent with Theorem 6.

(iii) Robustness of a QSPR descriptor

Theorem 7 guarantees that, as long as the deforming function $q(t)$

stays in the bounded class $\mathcal{Q}_1$ of Theorem 3, the deformed index cannot diverge for any finite molecular graph; this is a desirable stability property for a descriptor that is meant to be perturbed continuously rather than recomputed from scratch.

9 Conclusion

We have used the functional $q(t)-$ and $h(t)-$ calculus of Jafari and Manjarekar [5] to deform the vertex degree of a molecular graph through which every classical degree-based topological index. The resulting functional indices $\mathrm{TI}_{q(t)}(G)$ and $\mathrm{TI}_{h(t)}(G)$ converge to the classical index as $t \to 0$ and remain bounded for bounded deformation functions which are monotone in $q(t)$ under a mild positivity condition , and inherit a number-theoretic congruence structure directly from the degree sequence of the graph.

All of these results were confirmed numerically on the path, cycle, star and naphthalene molecular graphs in Section 6. While, Section 7 showed that an edge-weighted extension of the same substitution mechanism gives a genuine chemical application, tracking M_1 and M_2 continuously along the Diels–Alder reaction coordinate between their classical reactant and product values.

Declarations

During the preparation of this work, the author used AI-assisted technologies to generate the LaTeX code for the chemical representations in Section 7 and the formatting for Table 2.

References

[1] E. Deutsch, S. Klavžar, M-polynomial and degree-based topological indices, *Iranian J. Math. Chem.* **6** (2015) 93–102.

[2] E. Estrada, L. Torres, L. Rodríguez, I. Gutman, An atom-bond connectivity index: modelling the enthalpy of formation of alkanes, *Indian J. Chem.* **37A** (1998) 849–855.

[3] I. Gutman, N. Trinajstić, Graph theory and molecular orbitals. Total π-electron energy of alternant hydrocarbons, *Chem. Phys. Lett.* **17** (1972) 535–538.

[4] I. Gutman, Geometric approach to degree-based topological indices: Sombor indices, *MATCH Commun. Math. Comput. Chem.* **86** (2021) 11–16.

[5] H. Jafari, S. Manjarekar, A new concept of q-calculus with respect to another function, *J. Innov. Appl. Math. Comput. Sci.* **4** (2024) 113–121.

[6] V. Kac, P. Cheung, *Quantum Calculus*, Springer-Verlag, New York, 2002.

[7] M. Munir, W. Nazeer, S. Rafique, S. M. Kang, M-polynomials and topological indices of nanostructures, *Symmetry* **97** (2016) 1–12.

[8] M. Randić, Characterization of molecular branching, *J. Am. Chem. Soc.* **97** (1975) 6609–6615.

[9] J. Tariboon, S. K. Ntouyas, P. Agarwal, New concepts of fractional quantum calculus and applications to impulsive fractional q-difference equations, *Adv. Diff. Eq.* **18** (2015) 1–19.

[10] D. Vukičević, B. Furtula, Topological index based on the ratios of geometrical and arithmetical means of end-vertex degrees of edges, *J. Math. Chem.* **46** (2009) 1369–1376.

[11] H. Wiener, Structural determination of paraffin boiling points, *J. Am. Chem. Soc.* **69** (1947) 17–20.